

Detection Efficiency Of The CRIS Scintillating Optical Fiber Hodoscope

W.R. Binns¹, D.J. Crary¹, A.C. Cummings², L.Y. Geer¹, J. Klarmann¹, D.J. Lawrence¹, and R.A. Mewaldt²

1. Washington University, St. Louis, MO, USA; 2. Caltech, Pasadena, CA, USA.

ABSTRACT

Measurements of the detection efficiency of a Scintillating Optical Fiber Trajectory (SOFT) detector for 660 MeV/n Carbon, Boron, Beryllium and Lithium nuclei and for 300 MeV/n Fe nuclei are described. Detection efficiencies of 99.8%, 98.7%, 97.5%, and 93.8% for C, B, Be, and Li respectively were obtained for a single layer of fibers at an angle of incidence of 30°. These fibers had a black coating of extramural absorber (EMA) to optically decouple the fibers. Somewhat better detection efficiencies were obtained for optically coupled fibers (no EMA). The detection efficiencies for iron nuclei were $\geq 99.7\%$. We have used these results to estimate the event detection efficiencies of the fiber hodoscope which is planned for use in the Cosmic Ray Isotope Spectrometer (CRIS) (Stone, et al., 1989) experiment on the Advanced Composition Explorer (ACE). We find that for the highest energy Lithium nuclei which will stop in CRIS, the detection efficiency is about 89% for 6 plane events and about 99% for 5 plane events at 30°.

1. INTRODUCTION: Scintillating fibers have been developed by Washington University to perform precision trajectory measurements for charged particles. We have previously shown that a spatial resolution of about 60 μm can be obtained with a SOFT detector utilizing 200 μm scintillating fibers (Crary et al., 1992, and Davis et al., 1989) using iron nuclei. In the present paper we describe measurements taken at the LBL Bevalac to determine the detection efficiency (DE) of scintillating fibers as a function of both charge and angle for the lowest charged nuclei of interest to CRIS.

2. EXPERIMENT: In Dec., 1991 we exposed a test model of the SOFT hodoscope planned for use on CRIS to nuclei obtained from the LBL Bevalac. A cross-sectional view of the detector is shown in Fig. 1. The hodoscope consisted of three x,y planes of fibers (6 fiber layers) with the fiber outputs coupled to an image intensified CCD camera for readout as described in Crary et al., 1992. Fibers in each of the H1x, H1y, H2y, H3x, and H3y layers had no extra-mural absorber (no EMA), while the H2x fibers were individually coated with black ink (with EMA). A multi-wire proportional counter (MWPC) was placed in front of the SOFT detector to obtain an independent measurement of position and a plastic scintillator dE/dx detector (S) was placed behind the fibers to measure the charge of each particle. Two thin crossed scintillator paddles were used to generate an event coincidence. The SOFT detector was rotated so that measurements could be obtained for different beam incidence angles.

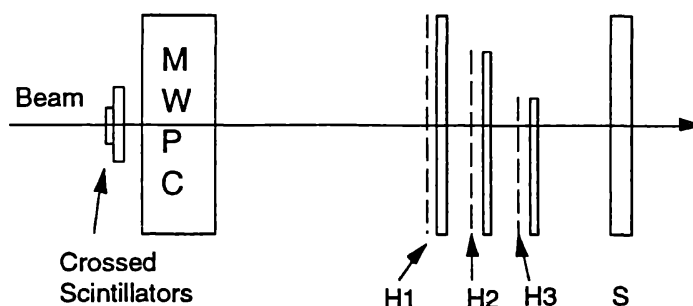


Fig. 1--Detector Cross-sectional View

Data were taken with beams of 660 MeV/n carbon and 300 MeV/n iron nuclei from the Bevalac. A polyethylene target was placed upstream of a bending magnet to interact the carbon beam and produce particles with lower charge. These particles were then steered onto our detector.

3. DATA ANALYSIS AND RESULTS: Fig. 2 shows a charge histogram from the dE/dx counter for the light nuclei analyzed in this test. A clean separation is observed for Li, Be, B, and C nuclei thus allowing us to clearly identify each particle and determine the detection efficiency as a function of charge. The analysis reported here is restricted to the three x-coordinate fiber layers. To be included in our analysis, we required that each event have good signals in the MWPC and in our dE/dx counter. To determine whether a particle was detected in a given layer we demanded a) a hit in the other two layers; b) that the position offset (Δx) in the layer of interest from a straight line connecting the points in the other two planes was within 4 standard deviations from the mean Δx for all particles of that charge; and c) the angle calculated using the three pixel cluster centroids was consistent with the mean angle within 4 standard deviations.

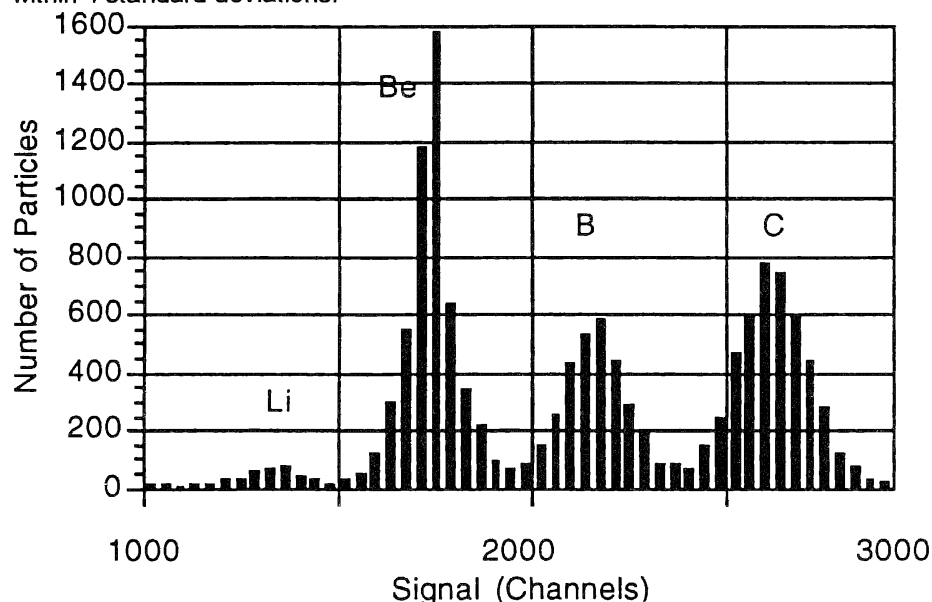


Fig. 2--Charge histogram from dE/dx counter.

In Fig. 3 we show the detection efficiencies for individual fiber layers plotted versus dE/dx for particle incidence angles of 0° , 15° , and 30° to the fiber plane normal and for a) fibers with EMA and b) fibers with no EMA. The data points correspond to 660 MeV/n Li, Be, B, and C nuclei as labeled above or below the data points. The curves labeled 1 and 2 correspond to a 30° incidence angle, 3 and 4 are for 15° , and 5 and 6 are for 0° . Curves 1, 3, and 5 are for fibers with no EMA and curves 2, 4, and 6 are for fibers with EMA. For all of these angles the fiber axis orientation was vertical and perpendicular to the beam direction.

We see that for all three incidence angles, the DE is better for fibers with no EMA. This was expected since the total amount of light collected by the camera is greater owing to coupling of the primary scintillator dye emission from the fiber traversed by the particle into adjacent fibers where the light is then waveshifted and lightpiped rather than being absorbed as would be the case for fibers with EMA. However the detection efficiencies are quite good even with EMA for 30° and 15° .

The decrease in DE for particles at 0° is not surprising since each $200\mu\text{m}$ fiber has an inactive acrylic cladding which is about $10\mu\text{m}$ thick. Thus we would expect a DE at 0° of about 90% if the cladding is totally inactive and there is no significant transport of energy into the scintillator by knock-ons created in the cladding. We note that the DE should be improved by fabricating fibers with thinner cladding.

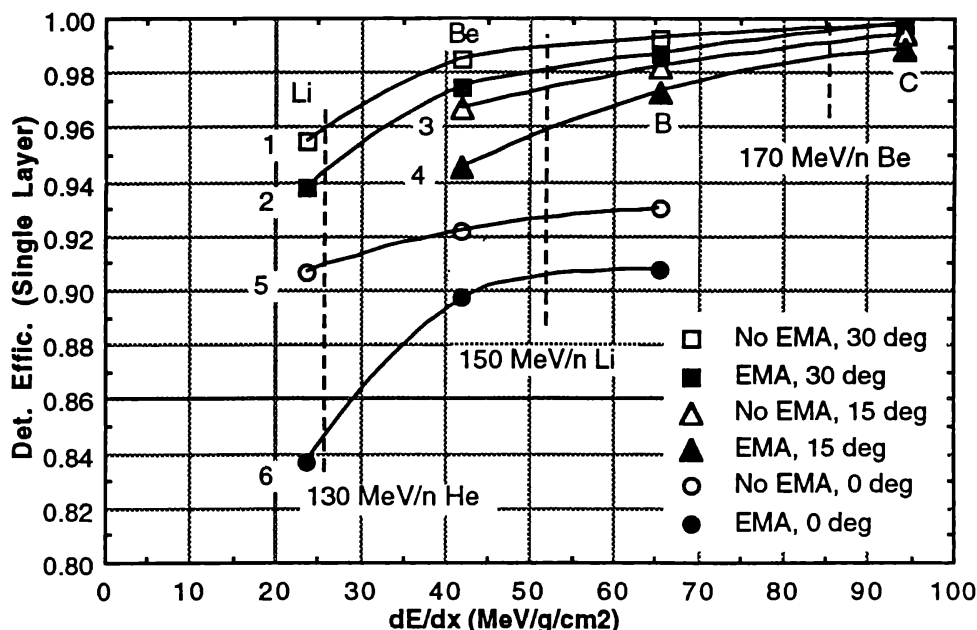


Fig. 3-Plot of single fiber layer detection efficiency vs. dE/dx for 660 MeV/n Li, Be, B, and C nuclei traversing fibers with no EMA (open symbols) and with EMA (closed symbols) for incidence angles of 0, 15, and 30 deg.

These measurements can then be scaled according to dE/dx to estimate the DE for elements with different energies than the 660 MeV/n beam energy. (This scaling is only approximately valid due to scintillator saturation). To show the implications for the detection efficiency on CRIS we have indicated by vertical dashed lines in Fig. 3 the dE/dx for the approximate highest energy (lowest dE/dx) stopping He, Li, and Be nuclei in the silicon detector stack (i.e. 130 MeV/n He, 150 MeV/n Li, and 170 MeV/n Be). We see that the detection efficiency for Li ranges from 90% to 99% depending upon the angle and whether EMA is used or not.

In Fig. 4 we show the hodoscope "event detection efficiency" which was calculated using the binomial distribution for our detector with 6 fiber layers. The left and right upper panels are for 30° and 15° incidence angles respectively, and the lower panel is for 0° . We see that the event DE for 6-layer events is greater than 89% for Li at 30° , and greater than 99% for 5-layer events. We note that the minimum requirement for the trajectory is 2-x and 2-y coordinates. These four coordinate events will have improved detection efficiency over those for 5 and 6 coordinate events. The 5th and 6th coordinates provide a redundant cross-check on the track.

We also exposed the same detector to iron nuclei with energy 300 MeV/n at incidence angles of 10° and 30° . For these highly ionizing nuclei, the single layer DE's were $\geq 99.7\%$.

4. CONCLUSIONS: We have measured the detection efficiency of single fiber layers, both with and without EMA, for 660 MeV/n Li, Be, B, and C nuclei and for 300 MeV/n Fe nuclei. The event detection efficiencies calculated from the single fiber layer efficiencies indicate that the SOFT detector on CRIS will have an excellent detection efficiency for Lithium and heavier nuclei.

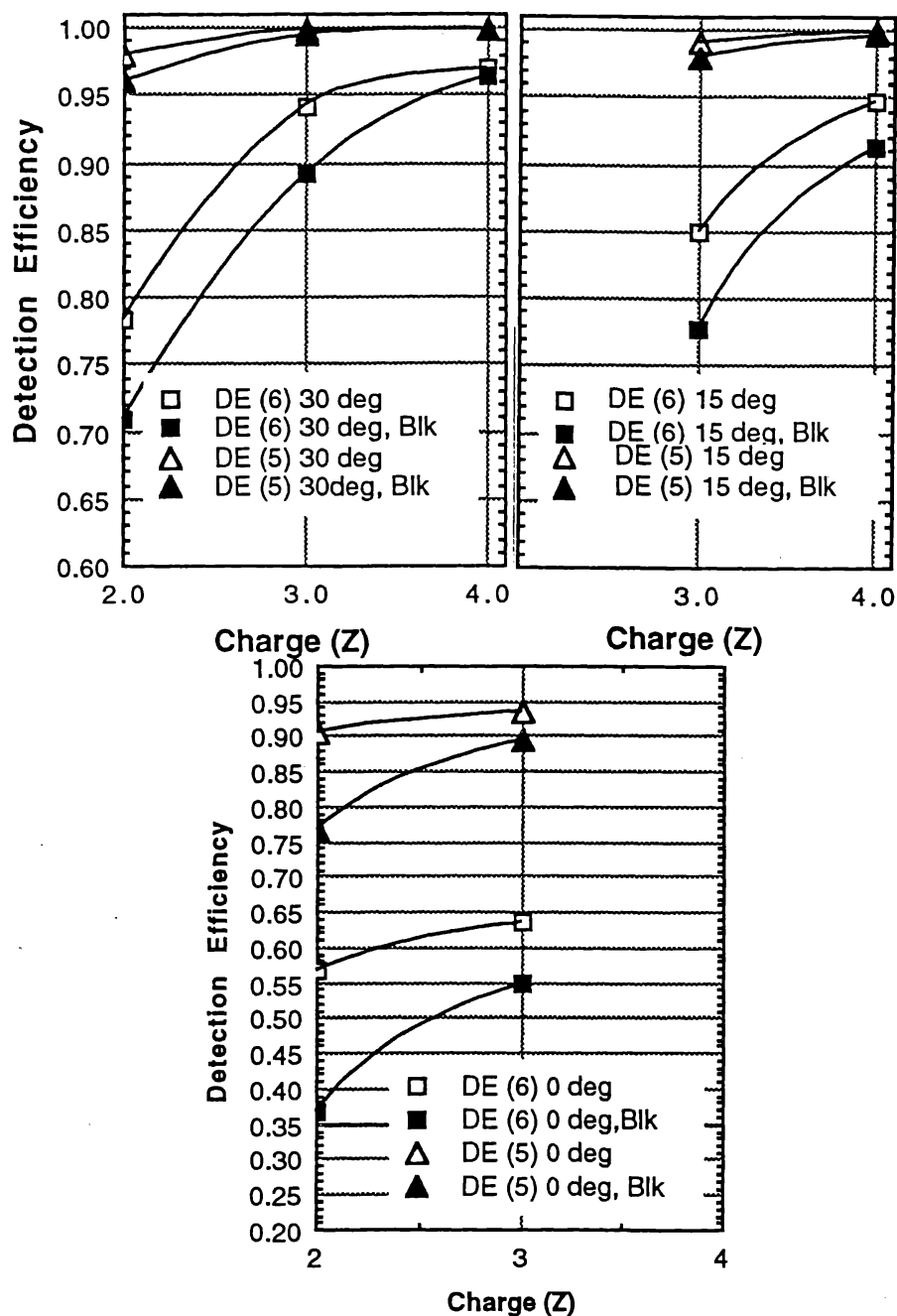


Fig. 4--Hodoscope event detection efficiencies for 6 layer and 5 layer events. The left and right top panels are for beam incidence angles of 30° and 15° respectively, and the lower panel is for 0°. These DE's are the worst case values for the highest energy (lowest dE/dx) of stopping particles.

REFERENCES

- Crary, D.J., et al., Nuclear Instruments and Methods, **A316** (1992) 311.
 Davis, A.J., et al., Nuclear Instruments and Methods, **A276** (1989) 347.
 Stone, E. C. et al., AIP Conference Proceedings, "Particle Astrophysics" **203** (1989)

ACKNOWLEDGEMENTS: This work was supported in part by NASA grants and in part by the McDonnell Center for the Space Sciences at Washington University.